General/Overview

RESEARCH IN SWEDEN ON DWELL IN CERAMICS

Patrik Lundberg
FOI, Swedish Defence Research Agency, Defence & Security Systems and Technology
SE-14725 Tumba, Sweden

ABSTRACT

The first documented high velocity tungsten long rod experiment in Sweden that clearly demonstrated the occurrence of dwell was conducted in 1987. In a set of impact experiments with different types of confined ceramic targets, one of the tests with a titanium diboride target showed a tremendous protection capability compared to the other targets tested. Post-mortem examinations showed that in this target, the tungsten rod had initially penetrated the ceramic in an ordinary way to a depth of some mm but then started to flow radially instead of continuing to penetrate through the sample. This single result was not possible to repeat and it was handled as an anomaly since the dwell phenomenon was not established at that time, and the experiment was soon forgotten. Ten years and over 200 dwell related experiments later, it is now well established that high velocity dwell and interface defeat is a result of the exceptional strength of the ceramics, and that this high strength is available if target damage can be suppressed. The major parts of the basic research in Sweden on dwell and interface defeat has been performed at FOI and focus has been on the loading conditions on the ceramic front face. Both stationary and non-stationary loading conditions relevant for an armour implementation have been analysed theoretically and studied experimentally in order to determine the performance limits of different ceramic materials.

INTRODUCTION

Initial studies on hard materials for armour applications started in Sweden during the fifties. At this time, geological materials like granite and diabas were tested for armour applications, primarily for protection against shape charge warheads. The first report on ceramics for protection against penetrating threats came in the late sixties and the first experiment with ceramic armour for protection against projectiles was made in 1973. The armour material at that time was an alumina used for electrical isolation which was produced in Sweden by IFÖ keramik AB.

During the early eighties, a special test facility with a smooth bored gun (calibre 30 mm) was set-up at FOA (later FOI) in order to facilitate systematic studies of the interaction between small scale long rod projectiles and various types of armours. An initial study of the protection capability of high quality ceramics was initiated 1986. The materials (Al_2O_3, Si_3N_4, B_4C, SiC and TiB_2) were produced by ASEA Cerama AB using a glass-encapsulated hot iso-static pressing technique to produce large samples of full dense materials.

The first documented high velocity tungsten long rod experiment that clearly demonstrated the occurrence of dwell was conducted in 1987. In a set of impact experiments at velocities of around 1550 m/s with different types of confined ceramic targets, one of the tests with a titanium diboride target showed a tremendous protection capability compared to the other targets tested. Post-mortem examinations showed that in this target, the tungsten rod had initially penetrated the ceramic in an ordinary way to a depth of some mm but then started to flow radially instead of continuing to penetrate through the sample. This single result was not possible to repeat and it was handled as an anomaly since the dwell phenomenon was not established at that

time, and the experiment was soon forgotten. Figure 1 shows the recovered ceramic from this specific test.

FIGURE 1. Post mortem examination of the titanium diboride "dwell target". The impact direction is from the top.

A ceramic armour consortium was formed by the Swedish Defence, Swedish ceramic industries and Swedish armour producers in 1990. The overall objective was to develop know-how for design and manufacture of weight and cost effective add-on ceramic armour for Swedish Military vehicles and vessels, especially for the CV-90 IFV. The program included basic as well as applied studies but, despite a large experimental program on the interaction between small and medium calibre projectiles and various types of ceramics lasting nearly four years, only one test indicating dwell was reported (a small scale experiment with titanium diboride).

The fist time dwell was investigated in an impact experiment in Sweden was in 1996. At this time information about the work by Hauver *et al.* had just reached Sweden and the first small scale reverse impact experiments with boron carbide targets were just to be conducted. Several of these experiments showed dwell to occur for considerable periods of time and although the initial idea of the experiments was not primarily to study dwell, these experiments opened for a Swedish research program on dwell and interface defeat. This effort is still continuing, but now with a smaller founding.

Ten years and over 200 dwell related experiments later, it is well established that high velocity dwell and interface defeat is a result of the exceptional shear strength of the ceramics, and that this high strength is available if target damage can be suppressed. The major parts of the basic research in Sweden on dwell and interface defeat has been performed at FOI (earlier FOA) and focus has been on the loading conditions on the ceramic front face. Both stationary and non-stationary loading conditions relevant for an armour implementation have been analysed theoretically and studied experimentally in order to determine the performance limits of different ceramic materials.

This paper summarises the work done at FOI on dwell and interface defeat for high velocity long rod projectiles impacting generic ceramic targets.

DWELL AND INTERFACE DEFEAT

Dwell and interface defeat was systematically studied and first reported by Hauver *et al.*[1,2] and later by Rapacki *et al.*[3]. They showed that by using different devices for load distribution and attenuation, including shrink-fitted or hot-pressed confinements, target damage could be suppressed. In this way it was possible to design thick ceramic armour systems capable of defeating long-rod projectiles at high impact velocities on the surface of the ceramic. This capability, named dwell or, if the threat was completely defeated, interface defeat, signifies that the projectile material is forced to flow radially outwards on the surface of the ceramic material without penetrating significantly. The mode of interaction is illustrated in Fig. 2 schematically as well as by a low velocity water jet and a flash X-ray picture from a high velocity impact experiment.

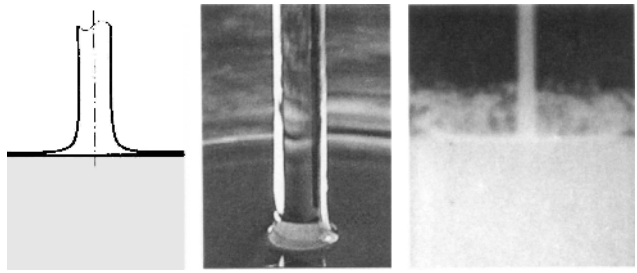

(a) (b) (c)

FIGURE 2. Dwell illustrated schematically (a), for a low velocity water jet (b) and for a high velocity tungsten long rod projectile (c) (flash X-ray picture).

The aim of the research at FOI was to estimate the transition velocity (i.e., the maximum velocity at which interface defeat can be maintained) at various loading conditions for different combinations of projectiles and ceramic targets. Another goal was to identify critical velocities which may serve as upper and lower bounds to the transition velocity, especially those related to the material properties of the projectile and the target.

In [4-7], the transition velocity was studied for different types of ceramic materials (boron carbide, silicon carbide, titanium diboride and Syndie) and in [8] it was estimated for one type of ceramic material (four grades of silicon carbide). The possibility to maintain dwell for a long period of time was studied in [9].

The influence of the properties of the projectile on the transition velocity was examined in [7] and [10]. In [7], use was made of two different projectile materials, a tungsten heavy alloy and molybdenum, with large difference in density. In [10] the transition velocity was estimated for a conical projectile and compared to that of a cylindrical projectile. In [11] the transition velocity of an unconfined target was studied.

In [7] the influence of the strength of the ceramic material on the transition velocity was studied using two models, viz., one for the surface pressure during interface defeat and one for the yield conditions in the ceramic material. The contact load during dwell at normal impact was further analysed in [12] and [13].

The constitutive models JH1 and JH2 by Johnson and Holmquist[14,15] were used to model the response of the ceramic material. JH1 was used in [10,12] under assumed conditions of interface defeat and JH2 was used in [5] to model both interface defeat and penetration.

EXPERIMENTAL TECHNIQUES

A two-stage light-gas gun was used for the impact experiments described in [4-9,11]. The pump-tube diameter of the gun is 80 mm and the diameter of the launch-tube is 30 mm. The impact experiments are performed in a tank connected directly to the launch tube. The experiments in [10] were performed with a 30 mm powder gun which has a similar impact tank and instrumentation as that of the light-gas gun. Figure 3 shows part of the light-gas gun facility.

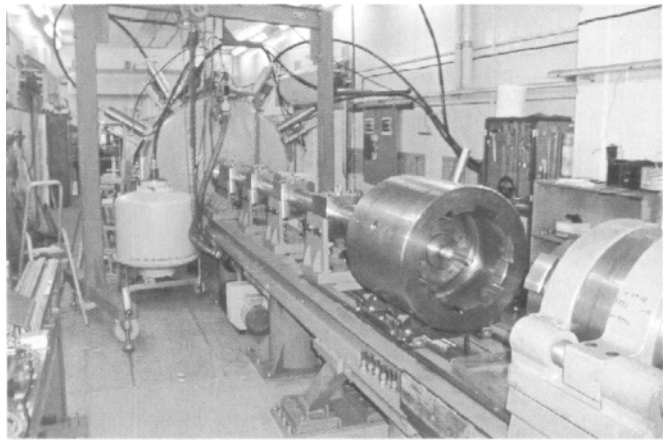

FIGURE 3. High pressure section, launch tube, impact tank and flash X-ray system of the two stage light-gas gun.

All the impact experiments were performed in a small scale with simple projectile and target geometries. Either the projectile was launched against a stationary target (direct impact) or the reverse impact technique was used. The latter means that the target is launched against the projectile, which is fixed in front of the muzzle of the launch tube. These two impact techniques are kinematically equivalent. Examples of projectile set-ups in reverse impact experiments are shown in Fig. 4.

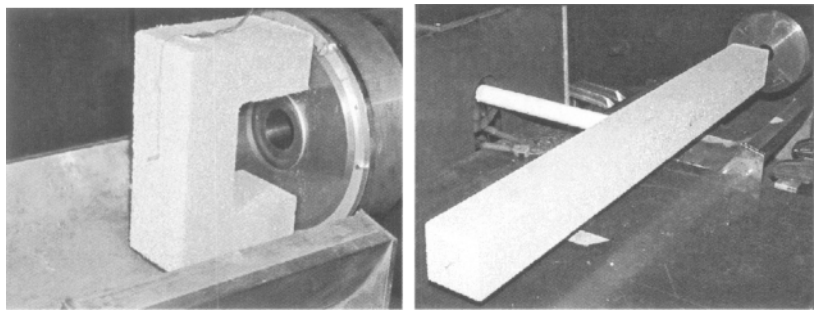

FIGURE 4. Examples of projectile set ups in reverse impact tests.

Several X-ray flashes (150 kV - 450 kV) were used to depict the penetration process. The flash X-ray technique makes it possible to see through the target and confinement materials. Therefore, it offered the possibility to study the penetration process in detail. An example of the X-ray set-up is shown in Fig. 5.

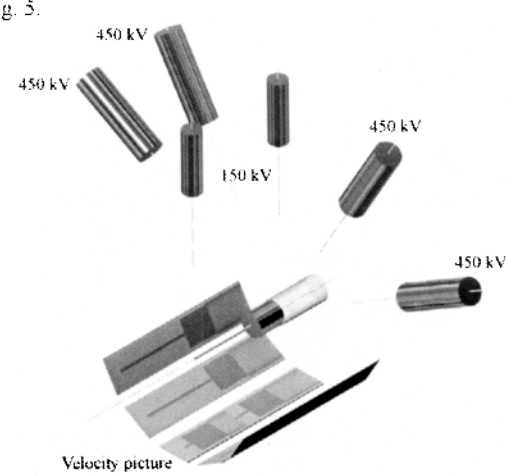

FIGURE 5. Typical X-ray set-up.

PROJECTILE AND TARGET MATERIALS USED

Two tungsten heavy alloys, DX2-HCMF from Pechiney and Y925 from Kennametal Hertel AG, were used as projectile materials. The ceramics used were produced by pressure assisted sintering (SiC-B, SiC-N, SiC-SC-HRN, SiC-HPN) and hot iso-static pressing (B_4C-AC, SiC-AC, TiB_2-AC). The diamond material in [7], Syndie, is a polycrystalline diamond composite produced by De Beers. In the reverse impact experiments, the projectile was mounted in front of the muzzle of the launch tube using either thin threads or a fixture of Divinycell. Two types of steel were used as confinement. Initially a tempered steel, SIS-2541-03, was used. This is comparable to AISI/SAE 4340. It was later replaced by a Maraging steel (Mar 350). The front cover was initially made of steel (2541-03), but later pure copper was used.

MODELLING AND ANALYSES

In [10], critical velocities related to the transition between interface defeat and penetration were determined for cylindrical and conical projectiles. Idealised loading conditions were used. Thus, the transient part of the loading and the influence of the radial growth of the surface load for the conical projectiles were not taken into account. The loading conditions are illustrated in Fig. 6.

The surface pressures and the corresponding critical velocities at which plastic yield is initiated at a point on the axis below the surface and the domain of plastic yield reaches the target surface were established in [7]. These states of yield, labelled incipient plastic yield (IY) and full plastic yield (FY), respectively, are illustrated schematically in Fig. 7.

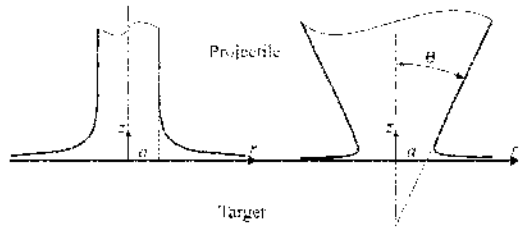

FIGURE 6. Flow of (a) a cylindrical and (b) a conical projectile during interface defeat.

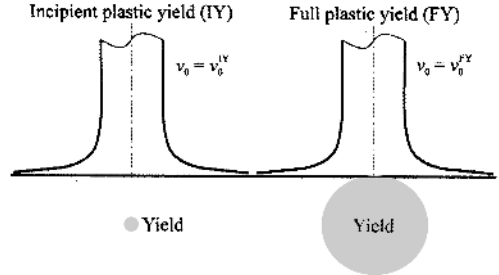

FIGURE 7. Critical levels of plastic yield used in [7]. (a) Incipient plastic yield (IY) and (b) full plastic yield (FY).

For a projectile with bulk modulus K_p, yield strength σ_{Yp} and density ρ_p, an approximate relation for the maximum surface pressure on the axis of symmetry was obtained as

$$p_s = q_p\left(1 + \frac{1}{2\alpha^2} + 3.27\beta\right), \qquad (1)$$

where $\alpha = K_p / q_p$, $\beta = \sigma_{Yp} / q_p$ and $q_p = \rho_p v_0^2/2$. Here v_0 is the impact velocity of the projectile and q_p is the stagnation pressure of an ideal fluid with density ρ_p and velocity v_0. The dimensionless parameters $\alpha >> 1$ and $\beta << 1$ relate elastic and plastic effects, respectively, to the effect of inertia. The modelling of the surface pressure was refined and expanded in [13], where the result (1) was confirmed.

The radial distribution of the surface pressure was approximated by a pressure profile determined experimentally for a low-velocity water jet. The assumed pressure distribution in combination with Boussinesq's elastic stress field solution gives the relation $p_0 = (2.601 + 2.056\nu)\tau_0$ between the maximum surface pressure p_0 and the maximum shear stress τ_0 in the ceramic. An approximate critical surface pressure corresponding to incipient yield (IY), was obtained by putting the maximum shear stress τ_0 equal to the shear yield strength τ_{Yc}.

A plastic slip-line solution for the indentation of a rigid punch into a rigid-plastic half-space was used to obtain an approximate critical surface pressure corresponding to full plastic yield (FY). According to this solution, the relation $p_{\text{mean}} = 5.70\tau_{Yc}$ between the mean pressure and the shear yield strength τ_{Yc} is valid. Here the mean pressure was taken as the maximum surface pressure, i.e. $p_0 = 5.70\tau_{Yc}$.

These critical surface pressures corresponding to incipient yield (IY) and full plastic yield (FY), give the approximate critical surface pressure interval

$$(1.30+1.03\nu)\sigma_{Yc} \le p_0 \le 2.85\sigma_{Yc}, \tag{2}$$

where $\sigma_{Yc} = 2\tau_{Yc}$ is the yield strength in uniaxial compression according to Tresca's hypothesis and ν is the Poisson's ratio of the ceramic. As relation (1) provides a relation between the maximum surface pressure p_0 and the impact velocity v_0, this relation and inequalities (2) give a critical velocity interval for the impact velocity v_0.

In [10], both cylindrical and conical projectile loading was studied by means of numerical modelling. The surface pressures and the corresponding critical velocities were established at which damage is initiated at a point on the axis below the surface, the domain of damage reaches the target surface, and a ring-shaped surface failure is initiated (damage and failure defined according to the Johnson and Holmquist constitutive models JH1 and JH2[14,15]).

These states of damage, labelled incipient damage (ID), full damage (FD) and surface failure (SF), are illustrated schematically in Fig. 8.

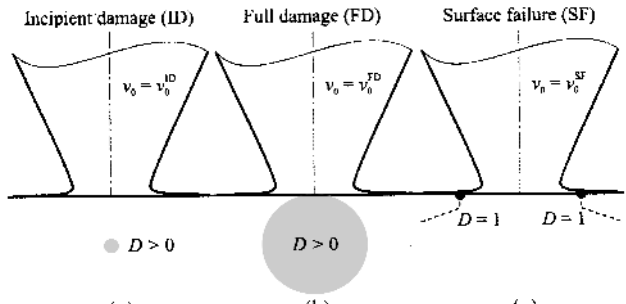

FIGURE 8. Critical levels of damage and failure used. (a) Incipient damage (ID), (b) full damage (FD) and (c) surface failure (SF). Reprinted from Reference [10] with permission from Elsevier.

The code Autodyn was used to determine the surface pressure on the target and the resulting target damage due to impact by conical and cylindrical projectiles. The simulations, two-dimensional with rotational symmetry, were carried out in two steps. In the first step, the pressure distribution on a flat, rigid and friction-free target surface was determined (Eulerian simulations, Johnson and Cook constitutive model [16]). In the second step, the surface pressure distribution was applied to a deformable target, and the damage of the target material was assessed (Lagrangian simulation, Johnson and Holmquist constitutive model JH1). Since each critical level of damage and failure corresponds to a critical surface pressure, it was possible to determine the critical impact velocities v_0^{ID}, v_0^{FD} and v_0^{SF}.

TRANSITION VELOCITY VERSUS MATERIAL PROPERTIES AND CONFINEMENT

For specific studies of the transition velocity, two slightly different targets were developed (designated Target A and B). For Target A, used in [7], the threaded front and back steel plugs were locked axially by rings which were electron-beam welded onto the tube. This was done in order to avoid early confinement failure. This target was used for estimations of the transition velocities for two grades of silicon carbide, titanium diboride and Syndie.

In order to facilitate the comparison of the transition velocity of materials with only small differences in mechanical properties, the target configuration was further developed. In particular, the front cover and the confinement tube were redesigned so that the transition velocity could be assessed in a more reproducible way. The increased simplicity of the target also facilitated modelling of dwell.

In this case, the confinement consisted of a thick-walled steel cup with a circular copper cover. The copper cover was expanded in its central part to a cylinder with diameter 4 mm and length 8 mm. It was glued onto the steel tube along the rim. This target (Target B) was used in [8] to determine transition velocities for four grades of silicon carbide, SiC-B, SiC-N, SiC-SC-1RN and SiC-HPN.

In order to study the influence of confinement on the transition velocity for SiC-B, a third unconfined target was used [11]. The copper cover was similar to the one used for Target B.

The geometries of Targets A, B and C are shown in Fig. 9.

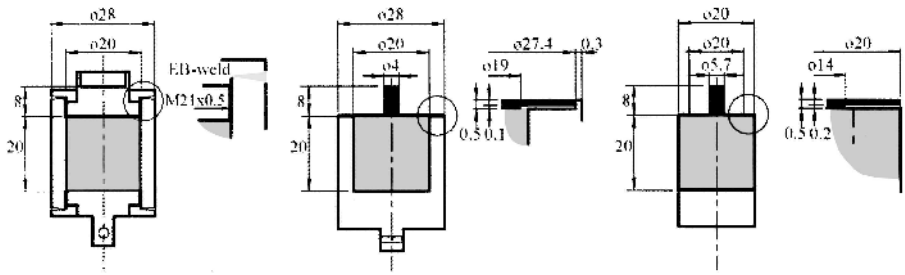

FIGURE 9. (a) Target A, (b) Target B and (c) Target C. Lengths in mm.

Yield strength of the target material

The transition velocity was determined for different types of ceramic materials (SiC-B, SiC-AC, TiB_2-AC, and Syndie) with relatively large variation in Vickers hardness. The Vickers hardness was used to estimate the yield strengths of the ceramics. Figure 10 shows the transition velocities determined from the impact experiments together with critical velocities corresponding to incipient yield (IY) and full plastic yield (FY). The critical velocities were determined from equation (1) and inequalities (2). The lower curve corresponds to Poisson's ratio $\nu = 0.07$.

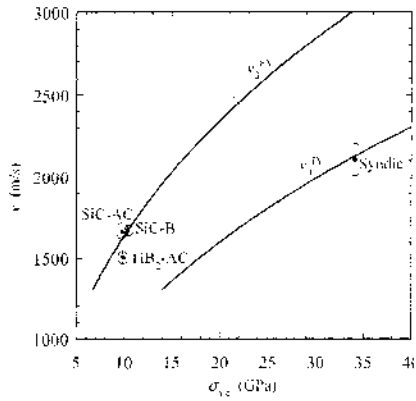

FIGURE 10. Transition velocity v_0^* from impact tests and critical velocities v_c^D, v_c^{CV} versus target yield strength σ_{Yc} (solid curves). The ends of the error bars represent the highest velocity without penetration ($\cup$) and the lowest velocity with penetration ($\cap$), respectively. Reprinted from Reference [7] with permission from Elsevier.

Fracture toughness of the target material

The transition velocity was determined for four grades of silicon carbide having relatively small variations in hardness and toughness. The transition velocities are plotted versus normalised hardness and toughness in Fig. 11.

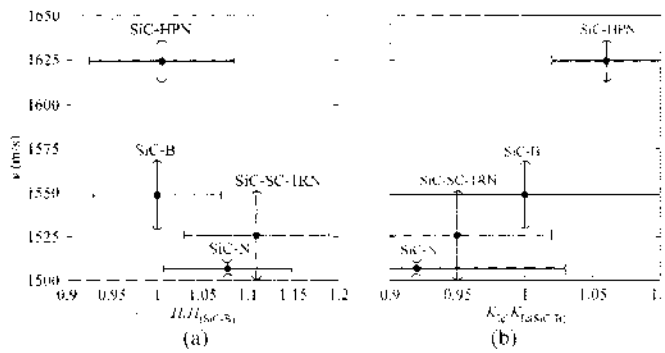

FIGURE 11. Transition velocity v_0^* versus (a) Vickers hardness H and (b) fracture toughness K_{Ic}. The lower and upper limits correspond to the highest velocity without penetration ($\cup$) and the lowest velocity with penetration ($\cap$), respectively. The left and right limits correspond to the standard deviation in hardness and fracture toughness. Reprinted from Reference [8] with permission from Elsevier.

Influence of the confinement

The transition velocity for one grade of silicon carbide (SiC-B) was determined for three different target designs representing different confinement conditions. The estimated transition velocities v_2^* are indicated as shaded areas in Fig. 12. The dashed curve in the figure is based on Tate's model.

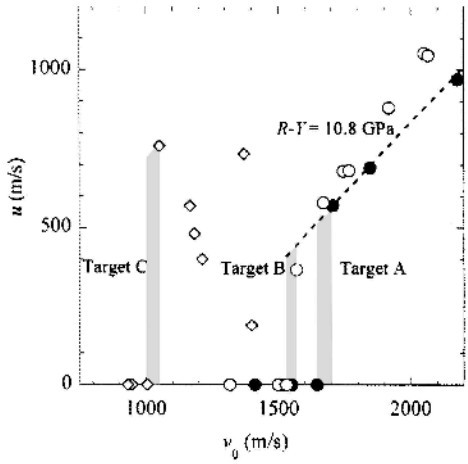

FIGURE 12. Penetration velocity u versus impact velocity v_0 in SiC-B for Target A (●), Target B (○) and Target C (◇). The shaded areas indicate transition regions. The dashed curve is based on Tate's model.

Density of the projectile material

Target A in Fig. 9 was used to study the influence of material properties of the projectile on the transition velocity. Two different projectile materials, a tungsten heavy alloy and molybdenum, with densities 17600 kg/m^3 and 10220 kg/m^3, respectively, were used. The observed intervals for the transition velocities are shown in Fig. 13 together with the penetration velocities estimated from Tate's model.

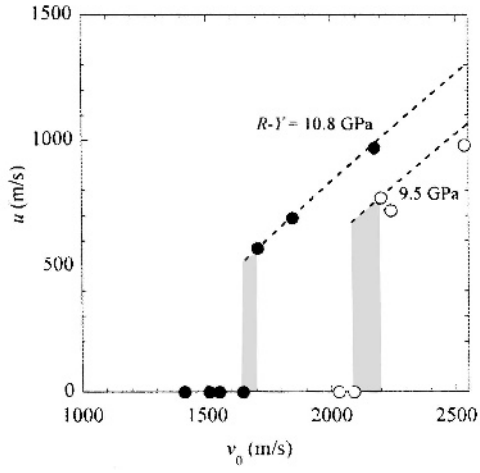

FIGURE 13. Penetration velocity u versus impact velocity v_0 for DX2-HCMF (●) and Mo (○) impacting SiC-B. The shaded areas indicate transition regions. The dashed curves are based on Tate's model.

TRANSITION VELOCITY VERSUS PROJECTILE GEOMETRY

In order to assess the influence of a conical nose shape on the transition velocity, experimental tests with conical and cylindrical WHA projectiles impacting silicon carbide targets were performed together with numerical simulations using the Autodyn code.

As pointed out above, the simulations were run in two steps. In the first, the surface pressures on the target were determined for different impact velocities under assumed condition of interface defeat. In the second, these surface pressures were applied to the target in order to obtain critical states of damage and failure related to the transition between interface defeat and penetration, see Fig. 8.

In the experiments, projectiles with cylindrical and conical fronts of nominal length 30 mm, fabricated by grinding sintered Y925 rods, were used. The conical front projectiles had apex angle 10° (half apex angle $\theta = 5°$).

The target consisted of a silicon carbide cylinder (SiC-B) shrink-fitted into a cylindrical steel cup. In the tests with the cylindrical projectiles and the conical projectiles with the larger front diameter, a small cylindrical copper cover was glued along its rim to the surface of the target. The geometries of the projectiles, the target and the copper cover are shown in Fig. 14.

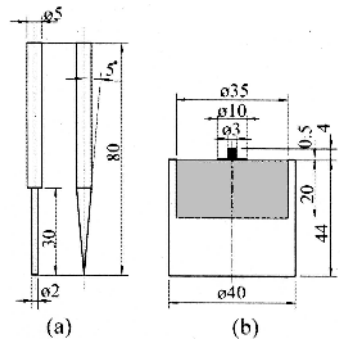

FIGURE 14. (a) Projectiles and (b) target with copper cover. Lengths in mm. Reprinted from Reference [10] with permission from Elsevier.

The dependence on half apex angle θ of the experimentally estimated transition velocity v_0^* and the calculated critical impact velocities v_0^{ID}, v_0^{FD} and v_0^{SF}, corresponding to incipient damage, full damage and surface failure, respectively, are shown in Fig. 15.

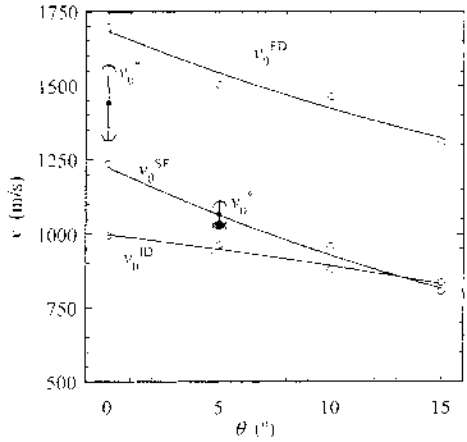

FIGURE 15. Transition velocity v_0^* from impact tests and critical velocities v_0^{ID}, v_0^{FD}, v_0^{SF} from simulations versus half apex angle θ. The ends of the error bars represent the highest velocity without penetration ($\cup$) and the lowest velocity with penetration ($\cap$). The solid curves are second-degree polynomial fits to the simulations ($\circ$). Reprinted from Reference [10] with permission from Elsevier.

DISCUSSION

In order to establish nearly quasi-static loading experimentally an attenuating device has to be used. In the FOI studies, this device was the front plug, initially made of steel, with a thickness sufficient enough to considerably reduce the initial transient load on the surface of the ceramic. This attenuation device was later changed to a copper cover that established erosion of the projectile before it reached the ceramic surface. During this process and the ensuing radial flow of the projectile material, the copper cover was eroded so that the projectile material was left unsupported on the target surface. The results in [8,9] show that after radial flow has been established, it continues steadily for a long time (several hundreds of micro seconds in [9]).

In [7], the surface pressures and the corresponding critical velocities were established at which plastic yield is initiated at a point on the axis below the surface and the domain of plastic yield reaches the target surface. These states of yield are shown as lower and upper critical velocities in Fig. 10. It can be noted that the estimated transition velocities in the experiments are close to these critical velocities.

In Fig. 11, SiC-N shows the lowest transition velocity, slightly above 1500 m/s, and SiC-HPN the highest, slightly above 1600 m/s. As the target configurations and impact conditions were the same in these tests, the difference between these transition velocities should depend on the mechanical properties of the ceramic materials. Furthermore, as the maximum surface pressure p_0 produced by the projectile during interface defeat is approximately proportional to the square of the impact velocity v_0 according to equation (1), i.e. $p_0 \propto v_0^2$, the 8% higher transition velocity for SiC-HPN than for SiC-N corresponds to a 16% higher maximum surface pressure. If the transition velocity v_0^* and the corresponding maximum surface pressure p_0^* are related to the shear yield strength τ_{Yc} of the ceramic material through $\tau_{Yc} \propto p_0^* \propto v_0^{*2}$ as proposed in [7], the strength of SiC-HPN should be about 16% higher than that of SiC-N. As can be seen in Fig. 11(a), however, the ranking in terms of hardness of the ceramic materials is not the same as that in terms of transition velocity. Actually, the hardness of SiC-HPN is 7% lower than that of SiC-N. This indicates that hardness alone, which reflects the shear yield strength, is not sufficient for estimating of the relative performance of ceramic materials in terms of transition velocities. Thus, the transition velocity cannot be controlled by plastic flow alone.

Figure 11(b) shows the transition velocity versus fracture toughness. Here, an increase in transition velocity corresponds to an increase in fracture toughness, although the uncertainty in fracture toughness is large. The maximum surface pressure is 16% and the fracture toughness 15% higher for SiC-HPN than for SiC-N. This observation indicates that, under the prevailing conditions, fracture may have more influence than plastic flow on the transition from interface defeat to penetration. As a consequence, the observed transition velocities may not be the maximum ones achievable. By suppressing of the initiation and propagation of cracks through increase of the confining pressure, it may be possible to increase the transition velocities.

The influence of confining pressure may be one reason for the difference in transition velocity between the three SiC-B targets used in Fig. 12. The target designs are shown in Fig. 9. Target A, with a front cover (and back plug) welded to the confining tube, gives 8% higher transition velocity as compared to Target B and 63% higher velocity as compared to Target C.

The influence of the material properties of the projectile on the transition and penetration velocities is shown in Fig. 13. The transition velocity intervals determined for a Tungsten projectile, DX2-HCMF, and a Mo projectile impacting SiC-B are indicated by grey zones. The assumption that the transition from interface defeat to penetration occurs at a critical surface pres-

sure gives $p^*_{Mo} = p^*_{WHA}$. Using of equation (1) and material data for DX2-HCMF and Mo then gives the relation between the transition velocities as $v^*_{Mo} / v^*_{WHA} \approx 1.34$. This agrees reasonably well with the experimental result $v^*_{Mo} / v^*_{WHA} \approx 1.28$.

In the tests with conical projectiles, the size of the copper cover was large compared to the initial diameter of the projectile tip. This means that the initial loading of the target surface was smoother than in the tests with cylindrical projectiles. Yet, the transition velocity for conical projectiles and copper-covered targets was significantly lower than that for the cylindrical projectiles for the same kind of target. The decrease of the critical velocities v_0^{ID}, v_0^{FD} and v_0^{SF} with increasing half apex angle θ observed in Fig. 15 is mainly an effect of the increase in the maximum surface pressure with this angle. For the cylindrical projectile ($\theta = 0°$), the magnitudes of these velocities and the experimentally determined transition velocity v_0^* are related as $v_0^{ID} = 990$ m/s $< v_0^{SF} = 1230$ m/s $< v_0^* = 1442$ m/s $< v_0^{FD} = 1690$ m/s. For the conical projectile ($\theta = 5°$) and copper-covered target, they are related as $v_0^{ID} = 960$ m/s $< v_0^{SF} = 1030$ m/s $\approx v_0^* = 1028$ m/s $< v_0^{FD} = 1500$ m/s. Thus, for the conical projectile the transition velocity is much lower relative to the three critical velocities than that of the cylindrical projectile, and it is close to the critical velocity v_0^{SF} associated with the formation of surface failure observed both in the experimental tests and in the simulations. This means that the difference in transition velocity between the cylindrical and the conical projectile is too large to be explained by the increased surface pressure alone.

The main reason for the different modes of penetration of cylindrical and conical projectiles, and the large difference in transition velocity, is believed to be the radial growth of the surface load from the conical projectile. This growth has the effect that cone-shaped surface cracks are exposed to the radial flow of projectile material under rising surface pressure. Therefore, when the pressure is sufficiently high, projectile material penetrates into the cracks as seen in the experiments.

CONCLUSIONS

The aim of the research at FOI was to estimate the transition velocity for various loading conditions and combinations of projectiles and ceramic targets and to identify critical velocities which may serve as upper and lower bounds for the transition velocity. These critical velocities have been related to the material properties of the projectile and the target.

The experiments show that there is a distinct transition from interface defeat to penetration. Possibly, there exists a unique transition velocity for each combination of projectile, target material and target configuration. Tests with different projectile materials (WHA and Mo) indicate that the transition occurs at a critical surface pressure.

The ceramic material with the highest hardness shows the highest transition velocity, 2110 m/s (Syndie), but for one type of ceramic material (four grades of silicon carbide), the ranking in terms of hardness is not the same as that in terms of transition velocity. This indicates that hardness alone, which reflects the shear yield strength, is not sufficient for estimation of the relative performances of ceramic materials in terms of transition velocities. It follows that the transition velocity cannot be controlled by plastic flow alone. Figure 11(b) shows that an increase in transition velocity corresponds to an increase in fracture toughness, although the uncertainty in fracture toughness measurement is large. This observation indicates that, for this target configuration, fracture may have more influence than plastic flow on the transition from interface defeat to penetration. As a consequence, the observed transition velocities may not be the maximum

ones achievable. By suppression of the initiation and propagation of cracks through increase of the confining pressure, it may be possible to increase the transition velocities for all materials tested.

The main reason for the different modes of penetration of cylindrical and conical projectiles, and the large difference in transition velocity, is believed to be the radial growth of the surface load from the conical projectile. This growth has the effect that the surface crack is exposed to the radial flow of projectile material under rising surface pressure. Therefore, when the pressure is sufficiently high, projectile material penetrates into the crack as seen in the experimental tests.

FUTURE RESEARCH

Even if the dwell phenomenon is well understood, some fundamental questions still needs further examination. In several of the studies at FOI, a complicated interaction between the flowing projectile material and macro-cracks has been observed at velocities close to the transition velocity. Infiltration of macro cracks by projectile material may enhance crack propagation substantially and contribute to the degradation of the ceramic target and thereby inhibit further dwell. This phenomenon is linked to the strong influence of the confining pressure on the transition velocity since the propagation of macro-cracks is sensitive to the confining pressure.

ACKNOWLEDGMENTS

This work was carried out at the Swedish Defence Research Agency FOI (former FOA), Weapons and Protection Division, as part of the research on long-rod projectiles and armour. The work was funded by the Swedish Armed Forces ([8] was also supported by the Army Research Laboratory (USA) through US Naval Regional Contracting Centre).

I would like to express my gratitude to my colleagues and especially to René Renström and Lars Westerling for their enthusiasm and will to share their knowledge at any time.

REFERENCES

1. G. E. Hauver, P. H. Netherwood, R. F. Benck and L. J. Kecskes. Ballistic performance of ceramic targets. *U. S. Army Symposium On Solid Mechanics*, USA (1993).
2. G. E. Hauver, P. H. Netherwood, R. F. Benck and L. J. Kecskes. Enhanced ballistic performance of ceramic targets. *19th. Army Science Conference*, USA (1994).
3. E. J. Rapacki, G. E. Hauver, P. H. Netherwood and R. F. Benck. Ceramics for armours- a material system perspective. *7th. Annual TARDEC Ground Vehicle Survivability Symposium*, USA (1996).
4. P Lundberg, L. Holmberg and B. Janzon. An experimental study of long rod penetration into boron carbide at ordnance and hyper velocities. *Proc 17th Int Symp on Ballistics*, South Africa; Vol 3, pp. 251-265 (1998).
5. L. Westerling, P. Lundberg and B. Lundberg. Tungsten long rod penetration into confined cylinders of boron carbide at and above ordnance velocities. *Int. J. Impact Engng*. 25. 703-714 (2001).
6. V. Wiesner, T. Wolf, P. Lundberg and Lars Holmberg. A study of the penetration resistance of titanium diboride using a new technique for time resolved terminal ballistic registrations. *Proc. 18th Int. Symp. on Ballistics*, USA, (1999).
7. P. Lundberg, R. Renström and B. Lundberg. Impact of metallic projectiles on ceramic targets: transition between interface defeat and penetration. *Int. J. Impact Engng*, 24, 259-275 (2000).
8. P. Lundberg, B. Lundberg, Transition between interface defeat and penetration for tungsten projectiles and four silicon carbide materials. *Int. J. Impact Engng*, 31, 781-792 (2005).
9. P. Lundberg, R. Renström, L. Holmberg. An experimental investigation of interface defeat at extended interaction times. *Proc. 19th. Int. Symp. Ballistics*, Vol. 3, 1463-1469 (2001).

10. P. Lundberg, R. Renström, B. Lundberg, Impact of conical tungsten projectiles on flat silicon carbide targets: transition from interface defeat to penetration. *Int. J. Impact Engng*, 32. 1842-1856 (2006).
11. O. Andersson, P. Lundberg, Rene Renström, Influence of confinement on the transition velocity of silicon carbide. *Proc. 23rd. Int. Symp. Ballistics*, Tarragona, Spain (2007) (to be published).
12. P. Lundberg, R. Renström, L. Westerling, Transition between interface defeat and penetration for a given combination of projectile- and ceramic material. In *Ceramic Armour by Design*, Edited by J.W. McCauley *et. al.*, Ceramic Transactions, Vol. 134 (2002).
13. R. Renström, P. Lundberg, B. Lundberg. Stationary contact between a cylindrical metallic projectile and a flat target under conditions of dwell. *Int. J. Impact Engng*, 30. 1265-1282 (2004).
14. T. J. Holmquist and G. R. Johnson. Response of silicon carbide to high velocity impact. *J. Appl. Phys.*, 91(9), 5858-5866 (2002).
15. G. R. Johnson and T. J. Holmquist. Response of boron carbide subjected to large strains, high strain rates and high pressure. *J. Appl. Phys.*, 85(12), 8060-8073 (1999).
16. G. R. Johnson and W. H. Cook. A constitutive model and data for metals subjected to large strains, high strain rates, and high temperatures. *Proc. 7th. Int. Symp. Ballistics*, 541-547 (1983).